Front. Mech. Eng. 2012, 7(3): 312–321
DOI 10.1007/s11465-012-0308-5

RESEARCH ARTICLE

Zhenyun DUAN, Houjun CHEN, Zhilan JU, Jian LIU

Mathematical model and manufacture programming of loxodromic-type normal circular-arc spiral bevel gear

Abstract In this paper, loxodromic-type normal circular-arc spiral bevel gear is proposed as a novel application of the circular-arc tooth profile at the gear transmission with intersecting axes. Based on the principle of molding-surface conjugation, the study develops a mathematical model for the tooth alignment curve and the computational flow at the design stage to enable the generation of the tooth surface. Machining of the tooth surface is then carried out to determine the interference-free tool path of the numerical control (NC). Moreover, a pair of loxodromic-type normal circular-arc spiral bevel gears is manufactured on computer numerical control (CNC) machine tools. The proposed theory and method are experimentally investigated, and the obtained results primarily reflect the superior performance of the proposed novel gear.

Keywords loxodrome, circular-arc tooth profile, Wildhaber-Novikov (W-N) gear, spiral bevel gear

1 Introduction

A helical gear with a circular-arc tooth profile in the gear drive with parallel axes was proposed by Wildhaber [1] and Novikov [2]. Since then, intensive research had centered on various aspects such as tooth geometry and optimization [3–6], contact and stress analysis [7–11], kinematics analysis [10], etc. In reality, a major difference exists between the ideas of these two inventors. The idea by Wildhaber was based on the generation of pinion and gear by the same imaginary rack cutter that provided a pair of line-contact tooth surfaces. On the contrary, Novikov's proposal was based on two mismatched imaginary rack cutters that generated a pair of point-contact tooth surfaces. In Novikov's study, the transverse section of the tooth surface was a circular arc in the theoretical analysis, whereas the normal section in practice is considered as a circular arc. Thus, the gear machining theory of Novikov departed from the kinematic theory he originally presented. Essentially, the ideas of Wildhaber and Novikov are similar. In the gear community, the gear type proposed by Wildhaber and by Novikov is still referred to as the Wildhaber-Novikov (W-N) gear. By using two mismatched rack cutters with parabolic profiles in internal tangency, Litvin et al. [12] proposed a new type of W-N gear that can effectively reduce noise and vibration caused by misalignment. Despite the numerous studies that had been conducted by scholars on W-N gear, it was only in 2001 that a study was conducted on the bevel gear with a circular-arc tooth profile. Kuo [13] proposed this kind of bevel gear and presented the ideal conditions of interference-free tooth surface using spherical geometry. Maiki and Watanabe [14] presented a method to manufacture a W-N spiral bevel gear on the machining center, conducted tooth contact analysis (TCA), and confirmed the results of TCA by the tooth contact mark obtained from the running-in experiment. Tsai and Hsu [15] investigated a kind of spiral bevel gear with a circular-arc contact path and tooth profile, derived the mathematical model for tooth geometry, and presented a machining method for general milling machine. Yao et al. [16] proposed the application of double circular-arc tooth profile in the nutation drive and developed a mathematical model of the tooth surface.

Spur gear, straight bevel gear, involute helical gear, and the W-N gear share some common characteristics. First, their conjugated tooth surfaces are molding surfaces [17] generated by sweeping the plane generatrix (i.e., the tooth

Received January 10, 2012; accepted March 20, 2012

Zhenyun DUAN
School of Mechanical Engineering, Shenyang University of Technology, Shenyang 110023, China

Houjun CHEN (✉), Zhilan JU
School of Mechanical Engineering, Nantong University, Nantong 226019, China
E-mail: mrchj365@ntu.edu.cn

Jian LIU
School of Mechanical Engineering, Dalian University of Technology, Dalian 116024, China

profile) along a directrix (i.e., tooth alignment curve) with a single degree of freedom (DOF). Second, the surface normals along the generatrix are coplanar in the normal plane of the directrix. Third, the instantaneous contact curve of tooth surfaces is always the generatrix. The gears mentioned above can be uniformly discussed under the principle of molding surface conjugation [18], which is different from the conventional theory of conjugate surfaces. More particularly, molding surface conjugation requires that the conjugated teeth are a pair of molding surfaces generated by the same generatrix, and that the instantaneous contact curve is always the generatrix. Hence, the conjugate relationship of tooth surfaces can be transformed into the relationship between the directrixes of tooth surfaces that involves the principle of molding surface conjugation. Following this principle, the gears with circular-arc tooth profile can be expanded into the intersecting-axis and the skew-axis drives, wherein the related theories have been presented in the literature [19]. Obviously, the W-N gear is only a special case of circular-arc tooth profile used for the convertibility of momentum between parallel axes. Its theory and technology have been developed.

In navigation, a line crossing all meridians of a longitude at the same angle is known as the loxodrome. In this paper, a curve cutting the generatrix on a given cone surface at a constant angle is also called the loxodrome. When a pair of conjugate loxodromes is chosen as the tooth alignment curves of tooth surfaces of gear and pinion, some advantages in the bevel gear with a circular-arc tooth profile are exhibited. As the spiral angle of the loxodrome is constant, machining the tooth surface on the numerical control (NC) machine tool using a milling cutter requires only two DOF that can be offered by any general milling machine. The ratio of the circumferential load, axial load, and the radial load of the tooth is constant, which gradually engages the gears to reduce the noise. According to the geometric characteristics of the tooth surface, this kind of bevel gear is called the loxodromic-type normal circular-arc spiral bevel gear (LCBG). LCBG is based on the following ideas. First, the directrixes of the tooth surfaces are a pair of loxodromes, whereas the generatrix is a circular arc in the normal section, which means that the tooth surface is a special illustration of the molding surface of the circular-arc generatrix. Second, LCBG follows the principle of molding surface conjugation. Lastly, the non-interference condition of the teeth is naturally satisfied.

As a practical application of the molding surface conjugation principle, this paper aims to present the design ideas and the mathematical model of the tooth alignment curve of the proposed LCBG by introducing crown gear as the intermediary conjugation between gear and pinion. On this basis, the method for generating the tooth surface on the computer numerical control (CNC) machine tool with the forming method is discussed, and the tool path that avoids the cutting interference is developed. Furthermore, the proposed theory and method are illustrated by a prototype of LCBG pair.

2 Mathematical model of LCBG

2.1 Basic idea

In the design and manufacture of the bevel gear, the complementary crown gear is an effective tool to derive the tooth surface of pinion and gear in which there is no exception. As to the generation of the LCBG pair, the crown gear with the circular-arc tooth profile is placed between the pinion and gear assembly. The center is located exactly at the intersection point of the pinion and gear shafts. Here, the directrix of the tooth surface of the crown gear is a loxodrome on the pitch plane and is an important token of tooth alignment. Hence, it is also called as the tooth alignment curve in this paper. When the pinion is located at the backside of the crown gear and meshes with the "negative teeth" while the gear is placed at the front side of the crown gear and meshes with the "positive teeth", kinematic coupling condition is fulfilled, which means that the pinion and gear can mesh with each other as well. Meanwhile, the pitch plane of the crown gear is simultaneously tangential with the pitch cones of gear and pinion. At the instantaneous axis, they roll without slipping with each other. In this process, an arc-length preserving map is formed, which can be utilized to obtain the tooth alignment curves of pinion and gear from the tooth alignment curve of the crown gear. The tooth alignment curve of the crown gear can map out a pair of conjugate tooth alignment curves of gear and pinion on respective pitch cones. As to the tooth alignment curves of the gear and pinion, they are always opposite with each other, but the spiral angles are equal.

In this paper, LCBG is considered to transfer the momentum between intersecting perpendicular axes. Some basic relationships between pinion, gear, and crown gear are considered, as demonstrated below

$$\begin{cases} r_c = \dfrac{r_1}{\sin\delta_1} = \dfrac{r_2}{\sin\delta_2},\ z_c = \dfrac{z_1}{\sin\delta_1} = \dfrac{z_2}{\sin\delta_2}, \\ \lambda_c = \lambda_1\sin\delta_1 = \lambda_2\sin\delta_2,\ I = \dfrac{z_1}{z_2} = \dfrac{\sin\delta_1}{\sin\delta_2}, \\ I_{1c} = \dfrac{z_1}{z_c} = \sin\delta_1,\ I_{2c} = \dfrac{z_2}{z_c} = \sin\delta_2, \end{cases} \tag{1}$$

where the subscripts "1", "2", and "c" indicate the pinion, the gear, and the crown gear, respectively, $r_i\,(i = 1,2,c)$ is the shortest distance from any coinciding point (conjugate point) of the tooth alignment curve to the respective rotating axis, $\delta_i\,(i = 1,2)$ is the pitch cone angle, $z_i\,(i = 1,2,c)$ is the number of teeth, $\lambda_i\,(i = 1,2,c)$ is the rotating angle, I is the speed ratio of pinion to gear, and I_{1c} and I_{2c} are the speed ratios between the crown gear and the pinion gear.

2.2 Determination of the tooth alignment curve

As previously mentioned, the tooth alignment curve reflects the direction of tooth alignment of LCBG. Hence, determination of the tooth alignment curve of the tooth is a chief task. According to the appointment, the tooth alignment curve of the crown gear of LCBG is a loxodrome on the pitch plane, which is a logarithmic spiral. From differential geometry, this spiral has the property wherein the angle between the tangent and the radial line at any point is constant.

As shown in Fig. 1, in the coordinate system $\{O_c;x_cy_c\}$ with the crown gear attached, the equation and the moving frame of the loxodrome C_p can be described as

$$\begin{aligned}
&\boldsymbol{R}_p = r_t\exp\left(\lambda_c\cot\overline{\beta_c}\right)\boldsymbol{E}(\lambda_c),\\
&\boldsymbol{e}_1 = \boldsymbol{E}\left(\lambda_c+\overline{\beta_c}\right) = \cos\left(\lambda_c+\overline{\beta_c}\right)\boldsymbol{i}_c + \sin\left(\lambda_c+\overline{\beta_c}\right)\boldsymbol{j}_c,\\
&\boldsymbol{e}_2 = \boldsymbol{E}_1\left(\lambda_c+\overline{\beta_c}\right) = -\sin\left(\lambda_c+\overline{\beta_c}\right)\boldsymbol{i}_c + \cos\left(\lambda_c+\overline{\beta_c}\right)\boldsymbol{j}_c,
\end{aligned} \tag{2}$$

where $\boldsymbol{R}_p$ is the radial vector, r_t is the inner cone distance, $\overline{\beta_c}$ is the nominal spiral angle, $\boldsymbol{e}_1$ and $\boldsymbol{e}_2$ are unit tangent and unit normal vectors, respectively, that form the moving frame, and $\boldsymbol{E}(\lambda_c)$, $\boldsymbol{E}\left(\lambda_c+\overline{\beta_c}\right)$, and $\boldsymbol{E}_1\left(\lambda_c+\overline{\beta_c}\right)$ are unit circle vectors.

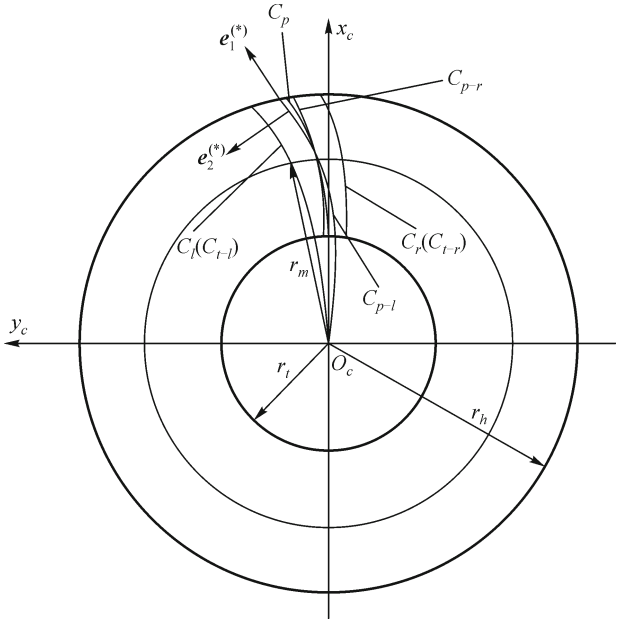

Fig. 1 Tooth alignment curve of the crown gear

By observing the generation of the molding surface, we find that an arbitrary point of the generatrix can trace the equidistant curve of the directrix. As a special illustration of the molding surface, the tooth surface of LCBG should have this property. In this case, once a tooth alignment curve is used to generate two flanks of "negative tooth" or "positive tooth" of the crown gear, the tooth thickness of the corresponding pinion and the space width of the corresponding gear become constant, resulting in the space width of the pinion, while the tooth thickness of the gear at the small ends becomes too big that the balance of the teeth bending strength is broken.

To avoid this problem, two separate tooth alignment curves should be derived to generate two flanks of tapered tooth: the left and the right flanks. Both flanks are obtained from the transformation of the nominal tooth alignment curve that is defined in Eq. (2). The left and the right tooth flanks of the crown gear are illustrated in Fig. 1. When the top surface of the tooth is upturned, from the small end to the big end, the two sides of the tooth are then called the left and the right flanks. In the following parts, the parameters with the subscripts "l" or "r" indicate their relation to the left or to the right flanks. To obtain the tapered tooth, we rotate the nominal tooth alignment curve C_p counterclockwise and clockwise with a small rotating angle $\Delta\lambda$ at the center axis of crown gear. The generated results C_{t-l}, C_{t-r} are chosen respectively as the left and the right theoretical borderlines of the tooth. According to the equidistant rule, C_p is adjusted as the actual left and right tooth alignment curves C_{p-l} and C_{p-r} at the mean pitch circle. Only in this way can their equidistant curves (actual borderlines of tooth) C_l, C_r can approach C_{t-l}, C_{t-r}.

According to above idea, for the theoretical borderlines C_{t-l}, C_{t-r}, their equations and moving frame can be described as

$$\begin{aligned}
&\boldsymbol{R}_t = r_t\exp\left(\lambda_c\cot\overline{\beta_c}\right)\boldsymbol{E}(\lambda_c\pm\Delta\lambda),\\
&\boldsymbol{e}_{t\text{-}1} = \boldsymbol{E}\left(\lambda_c\pm\Delta\lambda+\overline{\beta_c}\right),\\
&\boldsymbol{e}_{t\text{-}2} = \boldsymbol{E}_1\left(\lambda_c\pm\Delta\lambda+\overline{\beta_c}\right),
\end{aligned} \tag{3}$$

where the upper sign "+" and the lower sign "_" are used to express the theoretical left and right borderlines, $\boldsymbol{e}_{t\text{-}1}$ and $\boldsymbol{e}_{t\text{-}2}$ are unit tangent and unit normal vectors, and $\Delta\lambda$ is determined by the following equations:

$$\Delta\lambda = \frac{1}{2}q_0\gamma_c, \quad \gamma_c = \frac{2\pi}{z_c}, \tag{4}$$

where γ_c is the indexing angle of the crown gear and q_0 is the ratio of the indexing angle and the central angle that determines the tooth thickness. Generally, $q_0 = 0.618$.

For the actual tooth alignment curves C_{p-l}, C_{p-r}, their equation and moving frame can be uniformly represented as follows:

$$\begin{aligned}
&\boldsymbol{R}_p^{(*)} = r_t\exp(\lambda^*\cot\beta^*)\boldsymbol{E}(\lambda^*\pm\Delta\lambda),\\
&\boldsymbol{e}_1^{(*)} = \boldsymbol{E}(\lambda^*\pm\lambda_0^*+\beta^*),\\
&\boldsymbol{e}_2^{(*)} = \boldsymbol{E}_1(\lambda^*\pm\lambda_0^*+\beta^*),
\end{aligned} \tag{5}$$

where β^*, λ_0^* are the spiral and the starting angles, respectively, after the adjustment of C_p, λ^* is the rotating

angle parameter, and $\boldsymbol{e}_1^{(*)}$ and $\boldsymbol{e}_2^{(*)}$ are unit tangent and unit normal vectors. During computation, β^* and λ_0^* are substituted by β_l, λ_{0-l} of C_{p-l} and β_r, λ_{0-r} of C_{p-r}.

According to the definition of the equidistant curve, for actual borderlines C_l,C_r, their equation can be expressed as follow:

$$\begin{aligned}\boldsymbol{R}^{(*)} &= \boldsymbol{R}_p^{(*)} \pm r_0 \boldsymbol{e}_2^{(*)} \\ &= r_t \exp(\lambda^* \cot\beta^*)\boldsymbol{E}(\lambda^* + \lambda_0^*) \pm r_0 \boldsymbol{e}_2^{(*)},\end{aligned} \tag{6}$$

where r_0 is the radius of the working tooth profile, the upper sign "+" and the lower sign "−" are used to express the actual left and right borderlines C_l and C_r, respectively. With C_l as very close to C_{t-l}, they are denoted by the same curve in Fig. 1, while the same operation exists between C_r and C_{t-r}.

To ensure the rationality of the tooth size and the balance of the strength, the adjustment of C_p at the mean pitch circle satisfies the conditions that the magnitudes of $\boldsymbol{R}_t$ and $\boldsymbol{R}^{(*)}$ are equal to the mean cone distance r_m, while the lengths of their projections onto the vector $\boldsymbol{E}_1(\lambda_m^* \pm \lambda_0^*)$ are equal as well as their unit normal vectors. This condition can be expressed by the following equations:

$$\begin{cases} \boldsymbol{R}^{(*)^2} = \boldsymbol{R}_t^2 = \boldsymbol{r}_m^2, \\ \boldsymbol{R}^{(*)} \cdot \boldsymbol{E}_1(\lambda_m^* \pm \lambda_0^*) = \boldsymbol{R}_t \cdot \boldsymbol{E}_1(\lambda_m^* \pm \lambda_0^*), \\ \boldsymbol{E}_1\left(\lambda_m \pm \Delta\lambda + \overline{\beta_c}\right) = \boldsymbol{E}_1(\lambda_m^* + \lambda_0^* + \beta^*), \end{cases} \tag{7}$$

where the symbols with the subscript "m" indicate each of their relation to the mean pitch circle. By substituting Eqs. (3) and (6) into Eq. (7), the following expressions can be obtained:

$$\begin{cases} \lambda_m \pm \Delta\lambda + \overline{\beta_c} = \lambda_m^* + \lambda_0^* + \beta^*, \\ r_m \sin\left(\beta^* - \overline{\beta_c}\right) = \pm r_0 \cos\beta^*, \\ r_t \exp\left(\lambda_m \cot\overline{\beta_c}\right) = r_m, \\ [r_t \exp(\lambda_m^* \cot\beta^*) \mp r_0 \sin\beta^*]^2 + (r_0 \cos\beta^*)^2 = r_m^2. \end{cases} \tag{8}$$

Since $r_0, r_t, r_m, \overline{\beta_c}$ and $\Delta\lambda$ are known, the unknowns β^*, λ_0^*, λ_m^*, and λ_m can be solved as follows:

$$\begin{cases} \tan\beta^* = \left(\sin\overline{\beta_c} \pm \dfrac{r_0}{r_m}\right)\dfrac{1}{\cos\overline{\beta_c}}, \\ \lambda_m^* = \tan\beta^* \ln\left(\sqrt{\dfrac{r_m^2 - (r_0\cos\beta^*)^2}{r_t^2}} \pm \dfrac{r_0}{r_t}\sin\beta^*\right), \\ \lambda_m = \tan\overline{\beta_c} \ln\left(\dfrac{r_m}{r_t}\right), \\ \lambda_0^* = \lambda_m \pm \Delta\lambda + \overline{\beta_c} - (\lambda_m^* + \beta^*), \end{cases} \tag{9}$$

where the solutions with the upper sign "+" and the lower sign "−" are used for expressing C_{p-l} and C_{p-r}, respectively.

2.3 Determination of the tooth profile

As mentioned above, the basic tooth profile of LCBG in the normal section is a single circular arc, and its two sides are symmetric on the normal of the pitch cone or the pitch plane. In theory, the LCBG pair is in line contact, but the mismatch method is usually adopted to decrease the effect of errors, resulting in the tooth profile consisting of the working and the fillet circular arcs. For strength purposes, the convex profile is used for the pinion, and its radius is slightly smaller than that of the gear. Referring to the standard tooth profile of the W-N gear with a single circular arc, the sketch and the basic parameters of the tooth profile for LCBG are presented in Fig. 2 and Table 1.

Figure 2 describes a prototype of the tooth profile at the small end of the crown gear. In the practical generating process of the tooth, the centers of the two sides of the tooth profile move along the respective tooth alignment curve from the small end to the big end. Consequently, a tapered tooth is obtained.

2.4 Computational flow

The tooth profile and the tooth alignment curve have been identified and presented in Sections 2.2 and 2.3. The computational flow of the related parameters at the design stage of LCBG is accomplished as follows:

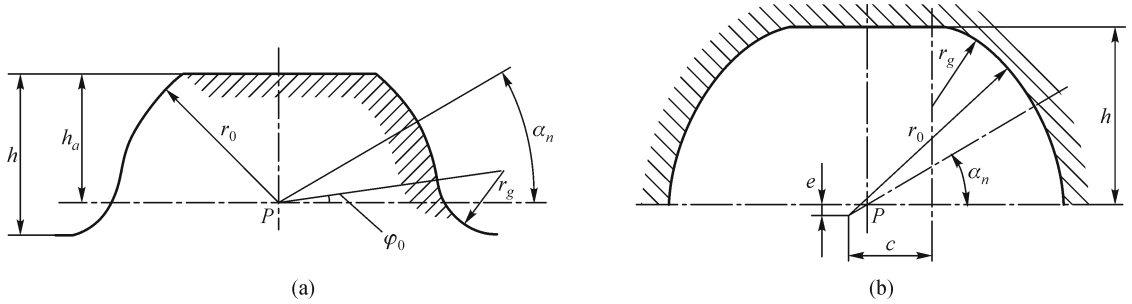

Fig. 2 Basic geometry of the tooth profiles. (a) Pinion; (b) gear

Table 1 Basic parameters of the tooth profile

Item	Symbol	Pinion	Gear
Pressure angle	a_n	30°	30°
Radius of the working profile	r_0	1.5 m_n	1.65 m_n
Addendum	h_a	1.2 m_n	0
Fillet radius	r_g	0.6248 m_n	0.6227 m_n
Tooth depth	h	1.5 m_n	1.36 m_n
Technological angle	φ_0	$8^\circ 47' 34''$	–
Transverse offset of the circular center	c	–	0.6289 m_n
Longitudinal offset of the circular center	e	–	0.075 m_n

Step 1 (Determining the nominal module and the nominal spiral angle). Nominal module m_n is chosen by the strength requirement, while the nominal spiral angle is generally $\overline{\beta_c} \leqslant 30^\circ$.

Step 2 (Determining the tooth number). Since the least tooth number of LCBG is not restricted by the interference condition [18], only the size and the strength are necessary to be considered in the design process. If the tooth number z_1 of the pinion is too large, the diameters of the gear and the pinion increase, while if it is too small, the tooth width increases. Hence, z_1 must be optimally chosen, and generally, $z_1 \geqslant 10$. Once z_1 is chosen, the tooth number z_2 of the gear can be obtained from the speed ratio. Besides, the pitch cone angles δ_1, δ_2 and the tooth number z_c of the crown gear can be acquired by Eq. (1).

Step 3 (Obtaining the pitch diameter at the small end). With the nominal module m_n defined at the small end of tooth, the pitch diameters D_{s1}, D_{s2} at the small ends of the pinion and the gear can be described as

$$D_{s1} = \frac{m_n z_1}{\cos\overline{\beta_c}},\ D_{s2} = \frac{m_n z_2}{\cos\overline{\beta_c}}. \tag{10}$$

The following inner cone distance r_t at the small end of the crown gear is then obtained

$$r_t = \frac{D_{s1}}{2\sin\delta_1} = \frac{D_{s2}}{2\sin\delta_2}. \tag{11}$$

Step 4 (Obtaining the pitch diameter at the big end and the tooth width). The contact ratio ε is firstly determined from the drive performance, and then the ending angle of the nominal tooth alignment curve at the big end of the crown gear can be specified as

$$\lambda_h = \varepsilon\gamma_c. \tag{12}$$

By substituting $\lambda_c = \lambda_h$ into Eq. (2) , the outer cone radius r_h at the big end of the crown gear is acquired

$$r_h = r_t \exp\left(\varepsilon\gamma_c \cot\overline{\beta_c}\right). \tag{13}$$

Subsequently, the pitch diameters D_{b1}, D_{b2} at the big ends of the pinion and the gear, as well as the tooth width b, can be derived as below:

$$D_{b1} = 2r_h\sin\delta_1,\quad D_{b2} = 2r_h\sin\delta_2,\quad b = r_h - r_t\,. \tag{14}$$

Step 5 (Obtaining the tooth profile). By substituting nominal module m_n into Table 1, the basic parameters of the tooth profiles for the pinion and the gear can be obtained.

Step 6 (Obtaining the parameters $\beta_l, \lambda_{0-l}, \beta_r, \lambda_{0-r}$ of the actual tooth alignment curves). By substituting the knowns, namely, $\overline{\beta_c}, r_t, r_0, r_m$ and $\Delta\lambda$ in Eq. (4) into Eq. (9), the parameters β_l, λ_{0-l}, and β_r, λ_{0-r} of the crown gear can be acquired.

According to the mapping relationship between the crown gear, the gear, and the pinion, the spiral angles of the gear and the pinion are equal to that of the crown gear, but their spiral hands are opposite to each other. Referring to Eq. (1), the starting angles of the left and the right tooth alignment curves of the pinion and the gear can be expressed as

$$\lambda_{1l} = \frac{\lambda_{0-l}}{\sin\delta_1},\ \lambda_{1r} = \frac{\lambda_{0-r}}{\sin\delta_1},$$
$$\lambda_{2l} = \frac{\lambda_{0-l}}{\sin\delta_2},\ \lambda_{2r} = \frac{\lambda_{0-r}}{\sin\delta_2}. \tag{15}$$

3 Manufacture programming of LCBG

For the tooth surface of LCBG, the surface normals along the tooth profile are coplanar. The tooth surface can be cut by using two methods: the generating method or the forming method. Only the forming method is discussed here. Meanwhile, the form-milling cutter is used. The knife-edge surface of the form-milling cutter is the torus surface formed by the tooth profile rotating on the cutter axis. The knife-edge surface and the tooth to be machined is a pair of conjugated molding surfaces that satisfy the principle of molding surface conjugation in the machining course and guarantee the accuracy of the tooth. The geometry of the tooth surface depends mainly on the tooth

alignment curve, based on the tool path programming developed at this section.

3.1 Geometric characteristics of the tooth alignment curve

According to Section 2.4 and in the literature [18], in the coordinate systems $\{O_1;x_1y_1z_1\}$ and $\{O_2;x_2y_2z_2\}$ with the pinion and the gear attached in Fig. 3, the equations and the moving frames of the tooth alignment curves $C_p^{(1)}$ and $C_p^{(2)}$ for pinion and gear, respectively, can be described as

$$\begin{aligned}
C_p^{(1)} : \boldsymbol{R}_p^{(1)} &= r_t\exp(\lambda_1\cot\beta^*\sin\delta_1)\\
&\quad [\sin\delta_1\boldsymbol{E}(-\lambda_1+\lambda_{01}^*)+\cos\delta_1\boldsymbol{k}_1],\\
\boldsymbol{e}_1^{(1)} &= \cos\beta^*[\cos\delta_1\boldsymbol{E}(-\lambda_1+\lambda_{01}^*)+\sin\delta_1\boldsymbol{k}_1]\\
&\quad -\sin\beta^*\boldsymbol{E}_1(-\lambda_1+\lambda_{01}^*),\\
\boldsymbol{e}_2^{(1)} &= -\sin\beta^*[\cos\delta_1\boldsymbol{E}(-\lambda_1+\lambda_{01}^*)+\sin\delta_1\boldsymbol{k}_1]\\
&\quad -\cos\beta^*\boldsymbol{E}_1(-\lambda_1+\lambda_{01}^*),\\
\boldsymbol{e}_3^{(1)} &= \cos\delta_1\boldsymbol{E}(-\lambda_1+\lambda_{01}^*)-\sin\delta_1\boldsymbol{k}_1,
\end{aligned} \tag{16}$$

$$\begin{aligned}
C_p^{(2)} : \boldsymbol{R}_p^{(2)} &= r_t\exp(\lambda_2\cot\beta^*\sin\delta_2)\\
&\quad [\sin\delta_2\boldsymbol{E}(\lambda_2+\lambda_{02}^*)+\cos\delta_2\boldsymbol{k}_2],\\
\boldsymbol{e}_1^{(2)} &= \cos\beta^*[\cos\delta_2\boldsymbol{E}(\lambda_2+\lambda_{02}^*)+\sin\delta_2\boldsymbol{k}_2]\\
&\quad +\sin\beta^*\boldsymbol{E}_1(\lambda_2+\lambda_{02}^*),\\
\boldsymbol{e}_2^{(2)} &= \sin\beta^*[\cos\delta_2\boldsymbol{E}(\lambda_2+\lambda_{02}^*)+\sin\delta_2\boldsymbol{k}_2]\\
&\quad -\cos\beta^*\boldsymbol{E}_1(\lambda_2+\lambda_{02}^*),\\
\boldsymbol{e}_3^{(2)} &= \cos\delta_2\boldsymbol{E}(\lambda_2+\lambda_{02}^*)-\sin\delta_2\boldsymbol{k}_2,
\end{aligned} \tag{17}$$

where $C_p^{(1)}$ is used to uniformly express two actual tooth alignment curves of the pinion, $\boldsymbol{e}_1^{(1)}$ is the unit tangent vector of $C_p^{(1)}$, and $\boldsymbol{e}_3^{(1)}$ is the unit normal vector of the pitch cone. Both $\boldsymbol{e}_1^{(1)}$ and $\boldsymbol{e}_3^{(1)}$ form the moving frame with $\boldsymbol{e}_2^{(1)}$. When we operate the left tooth alignment curve of the pinion, β^* is substituted by β_l, while λ_{01}^* is substituted by λ_{1l} which is computed in Section 2.4. When we operate the right tooth alignment curve of the pinion, β^* is substituted by β_r and λ_{01}^* is substituted by λ_{1r}. A similar operation can be applied to $C_p^{(2)}$ of the gear.

According to differential geometry, the geometric property of the curve can be represented by the curvature and the torsion. Using the derivatives of the unit vectors of moving frames in Eqs. (16) and (17) with respect to the arc-length parameter, the differential invariables of $C_p^{(1)}$, $C_p^{(2)}$ can be obtained as follows:

$$\begin{aligned}
\tau_g^{(1)} &= -\frac{\cos\beta^*\sin\beta^*}{r\tan\delta_1}, \quad \tau_g^{(2)} = -\frac{\cos\beta^*\sin\beta^*}{r\tan\delta_2},\\
k_n^{(1)} &= -\frac{\sin^2\beta^*}{r\tan\delta_1}, \quad k_n^{(2)} = -\frac{\sin^2\beta^*}{r\tan\delta_2},\\
k_g^{(1)} &= -\frac{\cos^2\beta^*\sin\beta^*}{r}, \quad k_g^{(2)} = -\frac{\cos^2\beta^*\sin\beta^*}{r},
\end{aligned} \tag{18}$$

where $r = r_t\exp(\lambda_1\cot\beta^*\sin\delta_1) = r_t\exp(\lambda_2\cot\beta^*\sin\delta_2)$ and $\tau_g^{(i)}$, $k_n^{(i)}$ and $k_g^{(i)}$ $(i=1,2)$ are the geodesic torsion, the normal curvature, and the geodesic curvature, respectively.

For a pair of conjugated tooth alignment curves, the absolute values of these invariables decrease with the increase in r, while $k_g^{(1)}$ is always equal to $k_g^{(2)}$. After the reciprocal operation of $k_n^{(i)}$ and $k_g^{(i)}$, the normal curvature radii $\rho_n^{(1)}$ and $\rho_n^{(2)}$, as well as the geodesic curvature radii $\rho_g^{(1)}$ and $\rho_g^{(2)}$ are acquired:

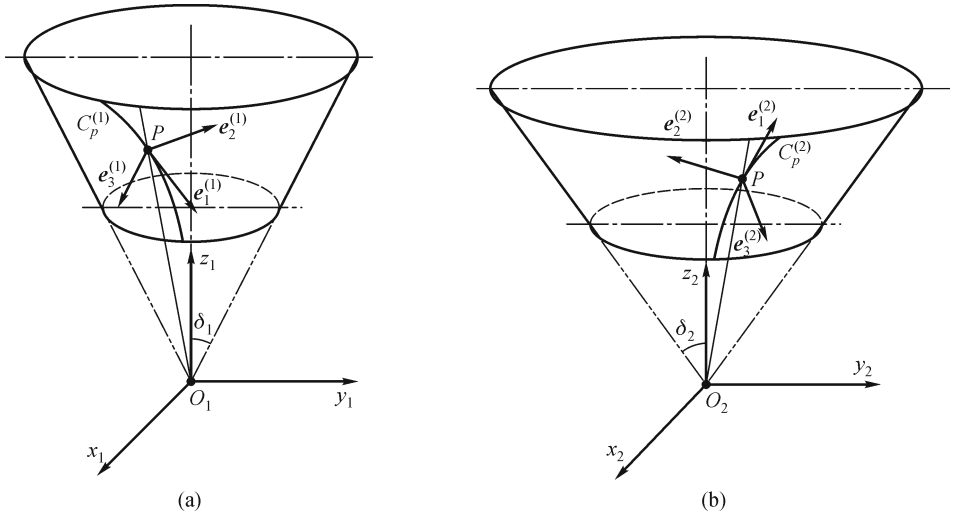

Fig. 3 Coordinate system. (a) Pinion; (b) gear

$$\begin{cases} \rho_n^{(1)} = -\dfrac{r\tan\delta_1}{\sin^2\beta^*}, \quad \rho_n^{(2)} = -\dfrac{r\tan\delta_2}{\sin^2\beta^*}, \\ \rho_g^{(1)} = \rho_g^{(2)} = -\dfrac{r}{\cos^2\beta^*\sin\beta^*}, \\ \dfrac{\rho_n^{(1)}}{\rho_g^{(1)}} = \text{const}, \quad \dfrac{\rho_n^{(2)}}{\rho_g^{(2)}} = \text{const}. \end{cases} \tag{19}$$

Obviously, $\rho_n^{(1)}$, $\rho_n^{(2)}$, $\rho_g^{(1)}$ and $\rho_g^{(2)}$ are linear with respect to r. They obtain the maximum at the big end and the minimum at the small end of the tooth, respectively. The normal curvature center $O_n^{(1)}$ and $O_n^{(2)}$ and the geodesic curvature center $O_g^{(1)}$ and $O_g^{(2)}$ can be denoted in the normal plane of the tooth alignment curve (see Fig. 5) with the aid of the operational method presented in the literature [19]. The line $\overline{O_n^{(1)}O_g^{(1)}}$ (or $\overline{O_n^{(2)}O_g^{(2)}}$) is the curvature axis of the tooth alignment curve $C_p^{(1)}$ (or $C_p^{(2)}$), while the distances of the point P to $O_n^{(1)}$ (or $O_n^{(2)}$) and $O_g^{(1)}$ (or $O_g^{(2)}$) are normal curvature and geodesic curvature radii, respectively. Since the ratio between $\rho_n^{(1)}$ and $\rho_g^{(1)}$ (or $\rho_n^{(2)}$ and $\rho_g^{(2)}$) is constant, the intersection angle of the curvature axis and the axis-$\boldsymbol{e}_2^{(1)}$ (or axis-$\boldsymbol{e}_2^{(2)}$) is also constant, which is favorable for the interference inspection.

3.2 Determination of the tool-path and the interference area

In the process planning for the workpiece machined by the forming method, determination of the relative position and the relative motion between the cutter and the workpiece is important. As shown in Fig. 4, the axis-z_1 (or axis-z_2) of the pinion blank (or gear blank) is inclined and forms the angle of $\pi/2-\delta_1$ (or $\pi/2-\delta_2$) with the axis-z_m of the machine tool setting and with the upper generatrix of the pitch cone as parallel to axis-x_m. Under the control of NC codes, the cutter axis is maintained in the normal plane of the tooth alignment curve and is always parallel to axis-z_m. In observing the motion from the small end to the big end, the pinion blank (or gear blank) rotates clockwise (or counterclockwise) on the axis-z_1 (or axis-z_2) with the rotating angle φ_1 (or φ_2). Relative to the workpiece, the cutter moves parallel along axis-x_m, and its motion is determined by the following equation

$$\begin{aligned} x_1 &= r_t\exp(\varphi_1\cot\beta^*\sin\delta_1), \quad \text{(for pinion)}, \\ x_2 &= r_t\exp(\varphi_2\cot\beta^*\sin\delta_2), \quad \text{(for gear)}. \end{aligned} \tag{20}$$

Since the spiral angle β^* is constant, changing the tool pose in the whole machining process is unnecessary. In general, the manufacture process only needs 2 DOF, namely, the rotation and the translation, that exhibit a good processing performance of LCBG. In order to achieve the point-contact, the center of the working tooth profile of the gear offsets from the tooth alignment curve with a constant distance, which is the difference of the radii of the working tooth profiles of gear and pinion. The trace of this center is a spatial equidistant curve of the tooth alignment curve of the gear. Since the difference of the radii is very small, an error generated from the machining principle is less than 1μm and can be ignored in the generation of the tooth.

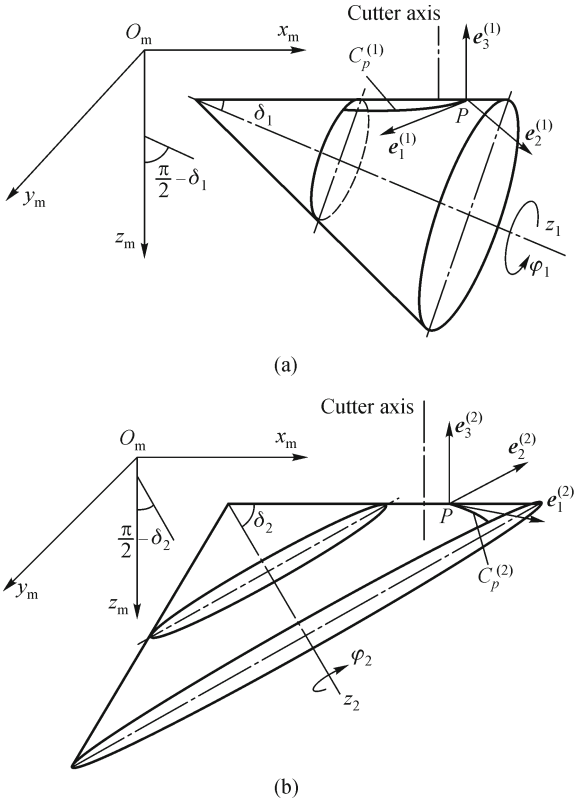

Fig. 4 Pose of blank on the worktable. (a) Pinion; (b) gear

In the machining course, curvature interference potentially exists. Since the knife-edge surface is a torus, the curvature axis of the directrix is the cutter axis. According to the interference condition, the line connecting the intersected point of the cutter axis and the curvature axis of the tooth alignment curve with the center of the working tooth profile intersects the tooth profile at the boundary points of interference. These points must be avoided in the machining area. As shown in Fig. 5, by connecting the center of the working tooth profile with the starting point a and the end point b of the working tooth profile, we can obtain two forbidden areas (the shadow parts). Hence, the non-interference condition for the machining can be represented as the intersected point of the cutter axis and the curvature axis of the tooth alignment curve outside the forbidden area.

With the interference condition coming from the general principle of the normal circular-arc gear [19], the tool pose is determined during tooth machining by the forming method. Figure 5 illustrates the tool pose of the

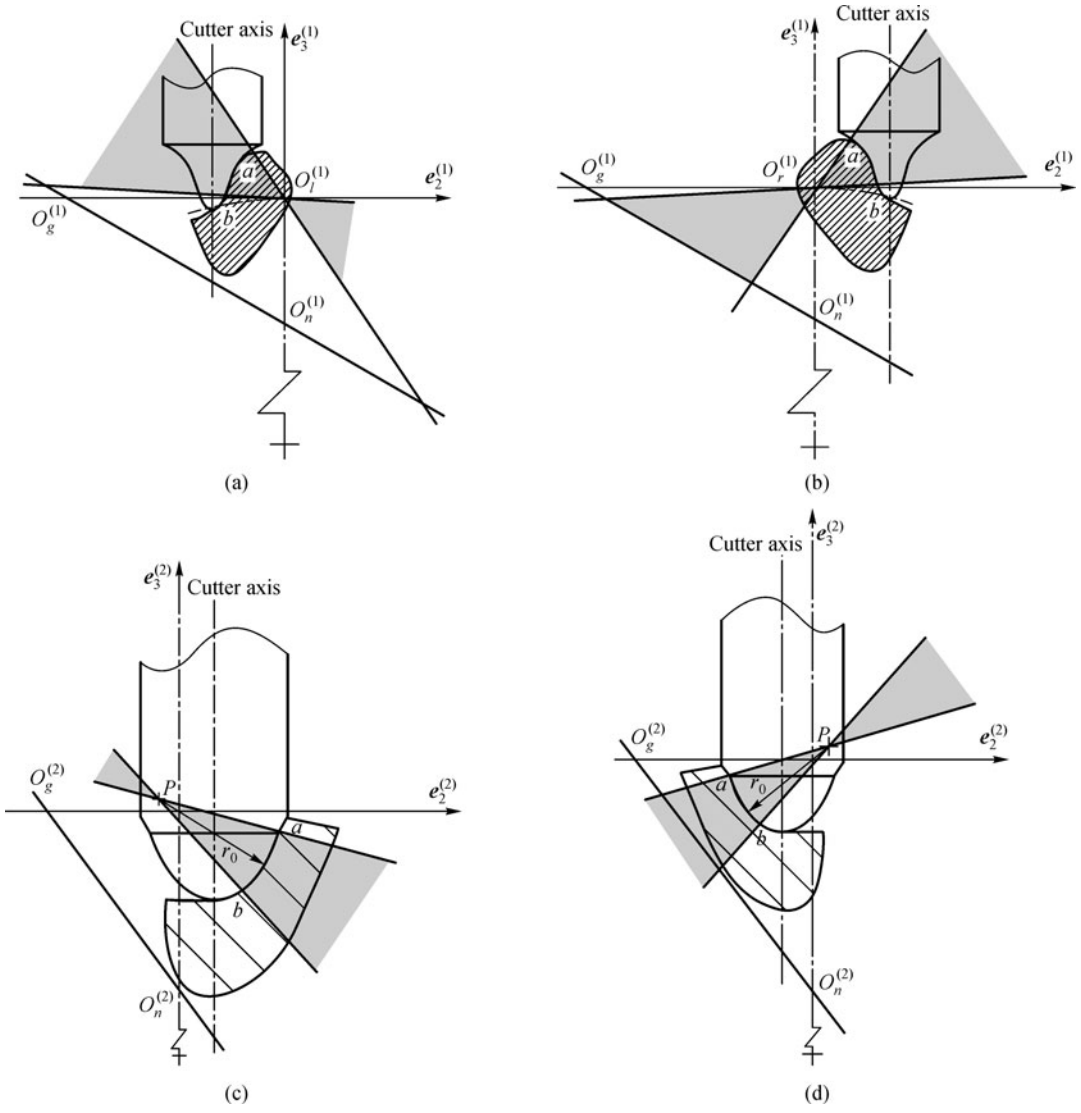

Fig. 5 Sketch of the interference area. (a) Left flank of pinion; (b) right flank of pinion; (c) left flank of gear; (d) right flank of gear

form-milling cutter and shows that the area fulfilling the non-interference rule is big.

4 Manufacture and running-in test of LCBG

The main purpose of the tests is to verify the proposed method and to conduct an elementary investigation on the running-in situation of the LCBG pair. The analyses are performed through the prototype machine of the LCBG pair using the design parameters in Table 2.

Figure 6 illustrates the machining process of LCBG on the CNC machine center with a pair of form-milling cutters. In the process of tooth cutting, the cutter is controlled by the NC codes programmed in terms of Eq. (20). Unlike the conventional method of spiral bevel gears, this method can machine any size of LCBG with the same module by a form-milling cutter. Certainly, for the manufacture of LCBG with the forming method, a relatively limited productivity is entailed.

The finished pinion and gear are installed on the test table, as shown in Fig. 7. The assembly is realized without intent to pursue the higher alignment accuracy. After 500 r/min and torque 30 N·m are applied to the pinion, the running test is conducted. By basic observation, the LCBG pair works very well and the level of noise is low. The contact pattern of the tooth flank is a continuous zonal area from the small end to the big end and occupies majority of the tooth-depth.

5 Conclusions

In this paper, LCBG was proposed as an application of the single circular-arc tooth profile at the intersecting-axes gear drive. The design idea of LCBG was presented, and

Table 2 Dimensions of the LCBG prototype

Item	Pinion	Gear
Tooth number	12	24
Hand of spiral	Left	Right
Nominal module	5 mm	
Shaft angle	90°	
Pressure angle	30°	
Nominal spiral angle	30°	
Contact ratio	2.1	
Inner cone distance	70.460	
Mean cone distance	125.832	

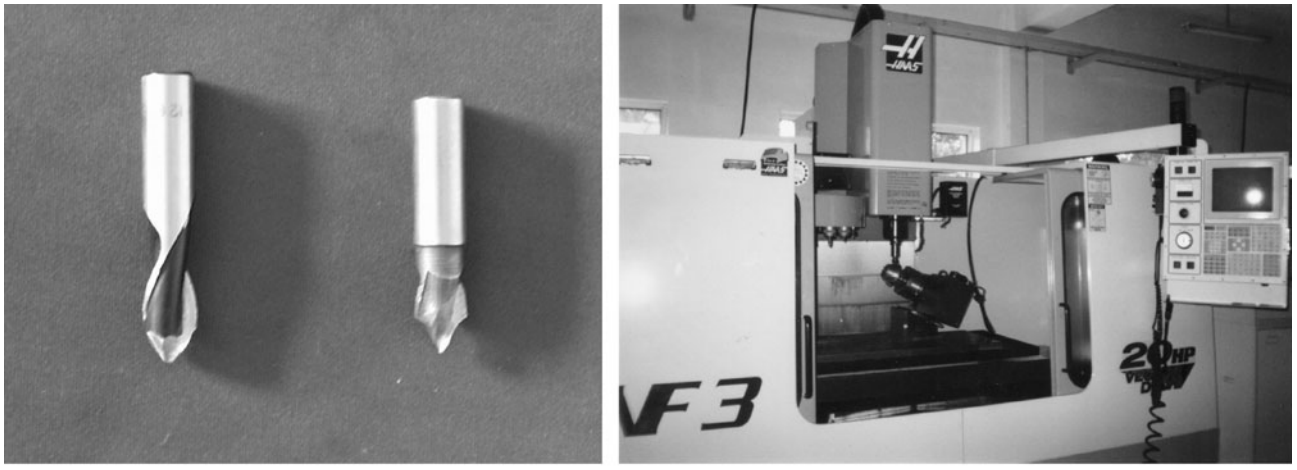

(a) (b)

Fig. 6 Photograph of NC machining experiment of LCBG. (a) From milling-cutter; (b) processing on NC machining center

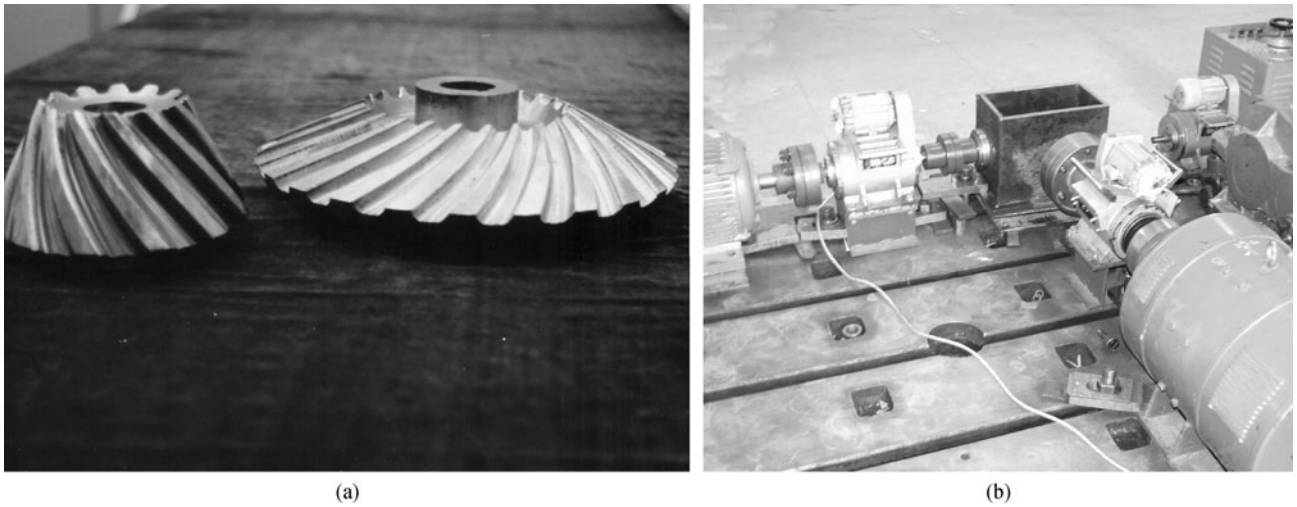

(a) (b)

Fig. 7 Running-in test of the LCBG prototype. (a) Pinion and gear; (b) test table

the mathematical models of the tooth alignment curve and the tooth profile were developed. Through the tooth alignment curve of the tooth surface, the tool path of tooth machining by the forming method was programmed, and the interference area was developed. The proposed theory and method were experimentally investigated. The obtained results primarily reflect the process and the contact performances of LCBG.

In our future work, the quantification of the contact pattern and transmission errors will be important topics.

Acknowledgements The work was supported by the National Natural Science Foundation of China (Grant No. 51105210) and by the Nantong University (Nos. 10ZY006 and 201010).

References

1. Wildhaber E. U.S. Patent, 1601750, 1926
2. Novikov M L. USSR Patent, 109750, 1956
3. Togashi S, Iyoi H. Improvement in W-N gears from the viewpoint of gear geometry-effects of mismatching or a difference in profile radii on the contact stresses. Mechanism and Machine Theory, 1973, 8 (3): 351–363
4. Lingaiah K, Ramachandra K. Photoelastic optimization of the profiles of Wildhaber-Novikov gears. Experimental Mechanics, 1976, 16(3): 116–120
5. Dyson A, Evans H P, Snidle R W. Wildhaber-Novikov circular arc gears: Geometry and kinematics. In: Proceedings of the Royal Society of London A, 1986, 403: 313–340
6. Ye G, Ye X Y. A new method for seeking the optimum gear tooth profiles–the theoretical basis of Wilhaber-Novikov gearing. Mechanism and Machine Theory, 2002, 37(10): 1087–1103
7. Maiki M. On the theory of the contact of the helical gear on the tooth normal plane. Transactions of the Japan Society of Mechanical Engineers, 1995, 61(582): 492–494
8. Tsay C B, Fong Z H, Tao S. Finite element stress analysis of Wildhaber-Novikov gears, In: Proceedings of 5th Conference on Mechanical Engineering, Taipei, 1988
9. Colbourne J R. The contact stress in novikov gears. Mechanism and Machine Theory, 1989, 24(3): 223–229
10. Tsay C B. Motion velocity of the contact ellipse over Wildhaber-Novikov gears. Journal of the Chinese Society of Mechanical Engineers, 1995, 16(2): 123–131
11. Litvin F L, Tsay C B. Helical gears with circular arc teeth: simulation of conditions of meshing and bearing contact. Journal of Mechanisms Transmissions and Automation in Design, 1985, 107 (4): 556–564
12. Litvin F L, Fuentes A, Gonzalez-Perez I, Carnevali L, Sep T M. New version of Novikov-Wildhaber helical gears: computerized design, simulation of meshing and stress analysis. Computer Methods in Applied Mechanics and Engineering, 2002, 191(12): 5707–5740
13. Kuo H M. A study on the bevel gear with circular-arc tooth profiles. Dissertation for the Master's Degree. National Sun Yat-sen University, 2001
14. Maiki M, Watanabe M. A study on WN spiral bevel gear manufactured by machining center, Journal of technological researches, 2005, 48(2): 91–97
15. Tsai Y C, Hsu W Y. The study on the design of spiral bevel gear sets with circular-arc contact paths and tooth profiles. Mechanism and Machine Theory, 2008, 43(9): 1158–1174
16. Yao L G, Gu B, Haung Sh J, Wei G, Dai J S. Mathematical modeling and simulation of the external and internal double circular-arc spiral bevel gears for the nutation drive. Journal of Mechanical Design, 2010, 132(2): 021008
17. Monge G. Application de l'Analysis à la Géometrie. Histoire de l'Acad, Des Sciences de Paris, 1850
18. Chen H J, Duan Z Y, Liu J, Wu H J. Research on basic principle of moulding-surface conjugation. Mechanism and Machine Theory, 2008, 43(7): 791–811
19. Chen H J, Duan Z Y, Wu H J, Liu J. Study on the general principle of normal circular-arc gear transmission. Mechanism and Machine Theory, 2006, 41(12): 1424–1442